# Stimulated Emission in Semiconductor Quantum Wire Heterostructures

E. Kapon, D. M. Hwang, and R. Bhat
*Bellcore, Red Bank, New Jersey 07701*
(Received 29 March 1989)

We report the first observation of stimulated emission in quasi-one-dimensional semiconductor quantum wires. Amplified spontaneous emission and stimulated emission spectra of the GaAs/AlGaAs quantum wires exhibit fine structure arising from transitions between lateral, one-dimensional electron and hole subbands. The observed subband separations, ~10 meV, are consistent with the calculated ones.

PACS numbers: 78.45.+h, 73.20.Dx, 78.60.Fi, 78.65.Fa

Quasi-one-dimensional (1D) or -zero-dimensional (0D) semiconductors, in which the charge carriers are quantum confined in two dimensions (2D) or three dimensions (3D), have attracted considerable attention recently. These so-called *quantum wire* and *quantum box* heterostructures are expected to exhibit larger electroabsorption and electrorefraction,[1] enhanced optical nonlinearities,[2] and higher differential optical gain[3] compared to more conventional semiconductors. In addition, quantum wires are expected to show unique electrical transport properties and to have extremely high electron mobilities.[4] Hence, considerable effort has been devoted to the fabrication and the experimental investigation of these structures.

The electrical transport properties of 1D and 0D heterostructures have been studied experimentally,[5,6] and effects associated with the higher degree of quantum confinement were reported. Optical effects due to the reduced dimensionality in these structures can be more difficult to interpret because of nonradiative recombination centers that are often introduced in the process of their fabrication. Fine structure in the spontaneous emission spectra arising from transitions between 1D or 0D electron and hole subbands,[7,8] resonant absorption between 1D subbands,[9] and optical anisotropy due to 2D confinement[10] were observed at low temperatures.

Here we report the first observation of stimulated emission in quasi-1D quantum wire heterostructures. The GaAs/AlGaAs quantum wires were fabricated using a novel heterostructure patterning technique[11] which results in near-ideal wire interfaces, thus allowing the generation of stimulated emission from 2D-quantum-confined carriers at room temperature. The 2D quantum confinement gives rise to fine structure in the amplified spontaneous emission spectra, indicating a lateral electron subband separation of ~10 meV. A model of the energy levels of the quantum wires, based on transmission electron microscopy (TEM) of the quantum wire cross sections, was found to be in agreement with the observed spectra.

Cross sections at the GaAs/AlGaAs quantum wire heterostructure are shown in Fig. 1. The structure was grown by organometallic chemical vapor deposition on a (100) GaAs substrate patterned with [01$\bar{1}$]-oriented V grooves, as described in detail elsewhere.[12] The AlGaAs cladding layers grow to form a very sharp corner between two {111} crystal planes. The active GaAs quantum well (QW), on the other hand, grows faster along the [100] direction, which results in the formation of a crescent-shaped QW at the bottom of the groove [see Fig. 1(b)]. As discussed below, this QW crescent provides the 2D quantum confinement for charge carriers injected at the *p-n* junction. The diode current was confined to the vicinity of the QW crescent by employing selective proton implantation [see Fig. 1(a)]. The graded $Al_xGa_{1-x}As$ regions next to the QW layer ($x$ is linearly graded from 0.2 near the QW to 0.5 at the $Al_yGa_{1-y}As$ boundary) serve as a dielectric waveguide for optical confinement.

The lateral tapering in the thickness of the QW crescent provides lateral variation in the effective band gap due to the increase in the carrier confinement energy

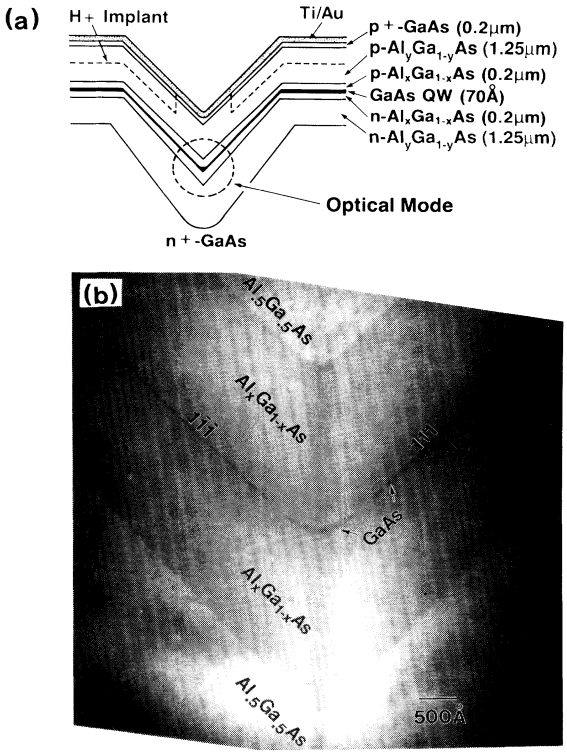


FIG. 1. Cross sections of GaAs/AlGaAs quantum wire heterostructure. (a) Schematic illustration; (b) dark-field transmission electron micrograph.

with decreasing QW thickness.[11] This lateral variation, in turn, results in a 2D potential well which confines the electrons and holes to a quasi-1D quantum wire. Since the effective band-gap variations due to the QW tapering are much more gradual than the transverse ones resulting from the Al-mole-fraction differences, it is possible to evaluate the 2D energy-level structure using a perturbation approach. Figure 2(a) displays the GaAs QW thickness obtained from the TEM cross section of Fig. 1(a) as a function of the lateral dimension $y$. The corresponding lateral variation of the confinement energy for electrons at the lowest QW level, $\epsilon_{el}(y)$, calculated in the effective-mass approximation using a finite-well model with $\Delta E_c/\Delta E_g = 0.6$, is shown in Fig. 2(b). The resulting lateral potential profile can be conveniently approximated by

$$U(y) = \epsilon_{el}(0) + \Delta\epsilon_{el} \tanh^2(y/2W), \quad (1)$$

where $\epsilon_{el}(0)$ is the confinement energy (due to the transverse band-gap variation) at the center of the crescent, $\Delta\epsilon_{el} \equiv \epsilon_{el}(\infty) - \epsilon_{el}(0)$, with $\epsilon_{el}(\infty)$ being the effective conduction-band edge far away from the center, and $W$ is a measure of the width of the potential well. The energy levels of (1), measured from the band edge of the bulk material, are given by[13]

$$E_{el,m} = \epsilon_{el}(0) + \Delta\epsilon_{el} - (\hbar^2/2m^*W^2)\{-(1+2m) + [1+(2m^*W^2\Delta\epsilon_{el}/\hbar^2)]^{1/2}\}^2, \quad m = 0,1,2\ldots, \quad (2)$$

where $m^*$ is the effective mass for electrons. Equation (2) shows that the QW tapering acts as a perturbation which splits the QW level of energy $\epsilon_{el}(0)$ into a set of lateral levels. The data of Fig. 2(b) are fitted by the potential profile approximation (1) with $\Delta\epsilon_{el} = 115$ meV and $W \approx 800$–$1000$ Å. The resulting 22 lateral electron levels are indicated in Fig. 2(b).[14] A similar procedure holds for evaluating the lateral hole levels. The total confinement energies for the lowest electron–heavy-hole and electron–light-hole transitions, assuming a $\Delta m = 0$ selection rule,[15] are 6.0, 17.8, 29.1, 40.0, 50.3,... and 8.5, 25.2, 41.1, 56.2, 70.4,... meV, respectively, for $m = 0,1,2,3,4,\ldots$.

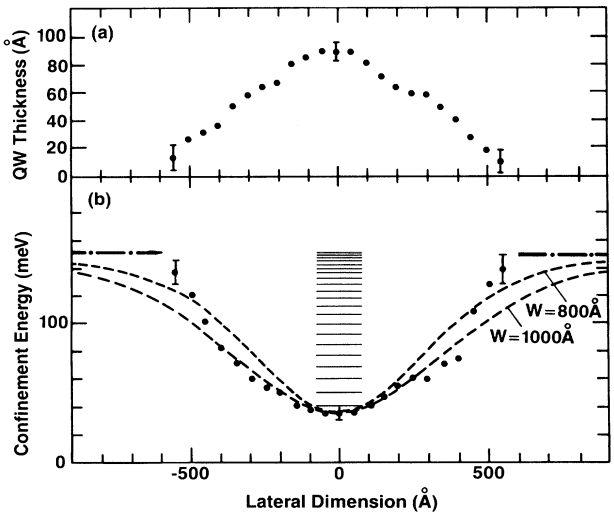


FIG. 2. (a) Thickness of the quantum well crescent vs the lateral dimension. (b) Confinement energy $\epsilon_{el}(y)$ for electrons at the lowest quantum well level vs the lateral dimension $y$ (solid circles). Dashed lines are model potentials calculated from Eq. (1) with $\Delta\epsilon_{el} = 115$ meV. Dashed-dotted lines indicate the $Al_{0.2}Ga_{0.8}As$ conduction-band edge. Lateral electron levels calculated from Eq. (2) are also shown.

Laser diode samples were fabricated from the quantum wire heterostructure described above by cleaving optical cavities of lengths ranging between $L = 0.25$ and 3.5 mm. The samples were excited under low-duty-cycle, pulsed conditions (400-nsec electrical pulses at 5 kHz) at room temperature. Emission spectra, observed from the cleaved ends, were measured using a grating spectrometer and a photomultiplier tube. The amplified spontaneous-emission spectra shown in Figs. 3(a) and 3(b) were obtained with quantum wire diode samples of cavity lengths of $L = 1.68$ and 0.54 mm, respectively. The spectrum shown in Fig. 3(c) is for a conventional QW laser diode structure in which the GaAs QW layer had a uniform thickness of (nominally) 70 Å.

Both quantum wire samples of Fig. 3 exhibit fine structure in their amplified spontaneous emission spectra, with peaks separated by ~8–10 meV. This spacing is consistent with the calculated separations between the quantum wire subbands within experimental error (see discussion below). The enhanced amplified spontaneous

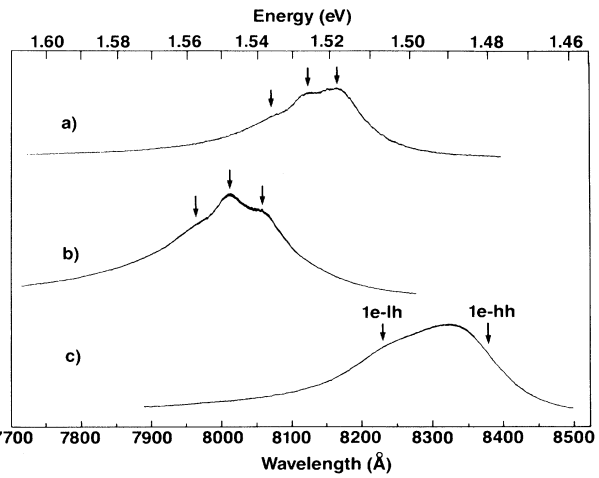


FIG. 3. Amplified spontaneous-emission spectra. (a) Quantum wire structure, cavity length $L = 1.68$ mm, diode current $I = 34$ mA. (Threshold current $I_{th} = 35$ mA.) (b) Quantum wire structure, $L = 0.54$ mm, $I = 17$ mA ($I_{th} = 18$ mA). Arrows indicate peaks due to transitions between the wire subbands. (c) Control quantum well sample with nominal QW thickness of 70 Å. The calculated ground-state electron–heavy-hole and electron–light-hole transitions for this thickness are indicated by the arrows.

emission at these peaks is a result of the larger density of states at the lateral subbands. From a simple rate-equation analysis it can be shown that the photon density $s$ inside the laser cavity is related to the rate of optical amplification $r_{gain}$ by $s = r_{spon}/(r_{loss} - r_{gain})$, where $r_{spon}$ is the spontaneous emission rate and $r_{loss}$ is the rate of optical extinction due to cavity losses. Thus, the increase in optical gain due to the higher density of states at the quantum wire subbands results in increased emission at the corresponding photon energies. This effect is enhanced close to threshold, when the rate of amplification $r_{gain}$ approaches that of the optical losses $r_{loss}$. Since the carrier Fermi levels become virtually clamped at lasing threshold due to the onset of stimulated emission, it is possible to observe only a part of the subband spectrum using this technique. However, the Fermi levels can be red shifted by increasing the optical cavity length because longer cavities result in lower mirror losses per unit length and, hence, lower carrier densities (lower gain per unit length) at threshold. As shown in Fig. 3, varying the cavity length allowed the observation of five lateral subband transitions for the quantum wire structures discussed here. The uniform-thickness QW structures, on the other hand, exhibited the expected spectra showing features due to 2D, ground-state electron to heavy-hole and electron to light-hole transitions [Fig. 3(c)].

Emission spectra obtained above the lasing threshold are displayed in Fig. 4. Near threshold ($I < 65$ mA), stimulated emission was observed at photon energies coincident with the lowest energy peak of the amplified spontaneous emission. At a higher diode current ($\sim 65$ mA) the lasing energy blue shifted abruptly by $\sim 6$ meV, corresponding to the separation between the peaks in the amplified spontaneous emission, which was $\sim 7$ meV (see Fig. 4). This "jump" in the lasing wavelength results from the gradual shift in the Fermi level which is not entirely clamped due to the finite amount of spontaneous emission coupled into the lasing mode. The discrete nature of the energy levels in the quantum wire leads to the multiple-peak structure in the gain spectrum and, hence, to the discontinuous change in the lasing wavelength. The higher-resolution spectra of Fig. 5 show finer structure resulting from interference of the coherent laser light inside the optical cavity. The envelopes of these spectra clearly display the enhanced gain at $\sim 1.54$ and 1.55 eV due to the larger density of states at the quasi-one-dimensional subbands.

Amplified spontaneous-emission spectra of quantum wire samples of cavity lengths between 0.25 and 3.5 mm exhibited peaks (as in Figs. 3–5) at photon energies of 1.515, 1.525, 1.537, 1.546, and $1.555 \pm 0.002$ eV. Stimulated emission was observed for each of these photon energies above threshold. The separations of these peaks, which were 10, 12, 9, and $9 \pm 4$ meV, respectively, agree within experimental error with the calculated transition energies for either electron to heavy-hole or electron to light-hole subbands with $m < 15$. Precise

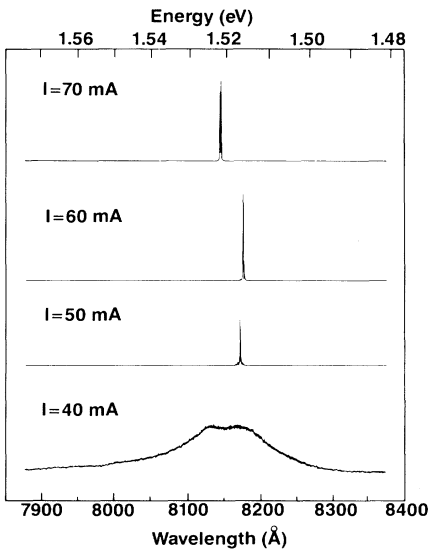


FIG. 4. Amplified spontaneous emission ($I = 40$ mA) and stimulated emission ($I = 50$, 60, and 70 mA) spectra from the quantum wire structure showing shifts between two adjacent lateral levels. Cavity lengths $L = 2.07$ mm; $I_{th} = 41$ mA.

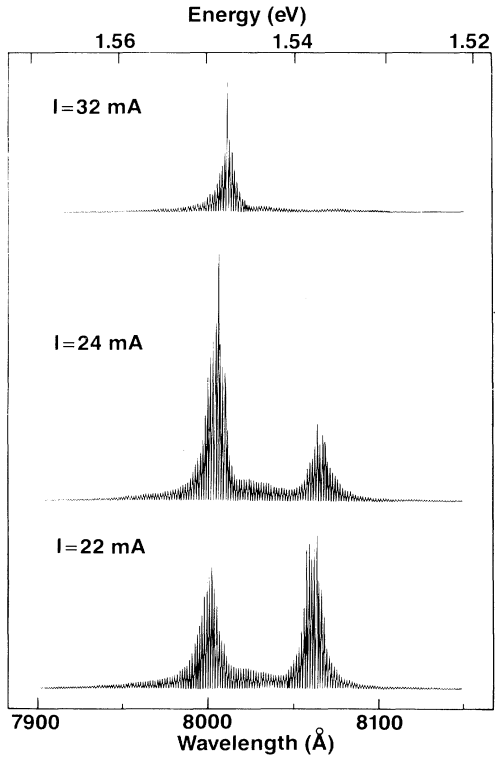


FIG. 5. Higher-resolution stimulated emission spectra for a quantum wire structure with cavity length $L = 0.54$ mm and threshold current $I_{th} = 18$ mA.

identification of the subbands participating in the stimulated emission, however, requires exact determination of the semiconductor band gap, including band-gap renormalization effects which are important at the high carrier densities near lasing threshold. Estimating a carrier density of $\sim 10^{18}$ cm$^{-3}$ and hence a band-gap shrinkage of $\sim 30$ meV (Ref. 16) we find that the lowest-lying subband observed in our structures corresponds to $m \cong 8$ for electron to heavy-hole transitions [$\epsilon_{el}(0) + \epsilon_{hh}(0) \approx 40$ meV] or $m \cong 4$ for electron to light-hole transitions [$\epsilon_{el}(0) + \epsilon_{lh}(0) \approx 60$ meV]. The relatively strong band-filling effects implied by these values of $m$ are due to the very small fraction ($\sim 10^{-3}$) of the optical intensity distribution which overlaps with the QW crescent. This small overlap leads to small effective model gains which, in turn, result in high carrier densities at threshold. Reducing the amount of band filling would result in stimulated emission from lower subband levels. This can be accomplished, e.g., by increasing the Al mole fraction $y$ (see Fig. 1) to improve the optical confinement, or by reducing the optical cavity losses in order to reduce the gain at threshold.

In summary, we reported the first observation of stimulated emission in quasi-one-dimensional semiconductor quantum wires. Amplified spontaneous emission and stimulated emission due to transitions between the quantum wire subbands were observed at room temperature. The measured energy separation of these subbands agrees with the predictions of a model based on high-resolution transmission-electron-microscopy analysis of the quantum wires. The demonstration of stimulated emission in quantum wire heterostructures adds an important aspect to the study of the optical properties of low-dimensional systems and opens new directions in the field of semiconductor lasers.

We wish to thank N. G. Stoffel for the proton implantation and C. P. Yun, L. Nazar, and M. A. Koza for technical assistance. Helpful discussions with S. J. Allen, D. E. Aspnes, K. Kash, T. P. Lee, P. F. Liao, and J. M. Worlock are gratefully acknowledged.

[1]D. A. B. Miller, D. S. Chemia, and S. Schmitt-Rink, Appl. Phys. Lett. **52**, 2154 (1988).

[2]S. Schmitt-Rink, D. A. B. Miller, and D. S. Chemla, Phys. Rev. B **35**, 8113 (1987).

[3]Y. Arakawa and A. Yariv, IEEE J. Quantum Electron. **22**, 1887 (1986).

[4]H. Sakaki, Jpn. J. Appl. Phys. **19**, 94 (1980).

[5]M. A. Reed, J. N. Randall, R. J. Aggarwal, R. J. Matyi, T. M. Moore, and A. E. Wetsel, Phys. Rev. Lett. **60**, 535 (1988).

[6]M. L. Roukes, A. Scherer, S. J. Allen, Jr., H. G. Craighead, R. M. Ruthen, E. D. Beebe, and J. P. Harbison, Phys. Rev. Lett. **59**, 3011 (1987).

[7]J. Cibert, P. M. Petroff, G. J. Dolan, S. I. Pearton, A. C. Gossard, and J. H. English, Appl. Phys. Lett. **49**, 1275 (1986).

[8]D. Gershoni, H. Temkin, G. J. Dolan, J. Dunsmuir, S. N. G. Chu, and M. B. Panish, Appl. Phys. Lett. **53**, 995 (1988).

[9]W. Hansen, M. Horst, J. P. Kotthaus, U. Merkt, Ch. Sikorski, and K. Ploog, Phys. Rev. Lett. **58**, 2586 (1987).

[10]M. Tsuchiya, J. M. Gaines, R. H. Yan, R. J. Simes, P. O. Holtz, L. A. Coldren, and P. M. Petroff, Phys. Rev. Lett. **62**, 466 (1989).

[11]E. Kapon, M. C. Tamargo, and D. M. Hwang, Appl. Phys. Lett. **50**, 347 (1987).

[12]R. Bhat, E. Kapon, D. M. Hwang, M. A. Koza, and C. P. Yun, J. Cryst. Growth **93**, 850 (1988).

[13]L. D. Landau and E. M. Lifshitz, *Quantum Mechanics* (Pergamon, Oxford, 1977), 3rd ed., p. 73.

[14]We consider only the ground (unperturbed) state of the quantum well. A second, higher-energy state for electrons exists for QW thickness $> 70$ Å. However, the confinement energy of this state, 120 meV at 90-Å thickness, is large enough so that it does not affect lateral levels originating from the ground QW state with $m < 11$; see, e.g., J. A. Burn and G. Bastard, Superlattices Microstruct. **4**, 443 (1988).

[15]This selection rule holds only approximately in our case since the lateral potential wells for different types of carriers have different shapes.

[16]H. Kressel and J. K. Butler, *Semiconductor Lasers and Heterojunction LED's* (Academic, New York, 1977), Chap. 3, p. 91.

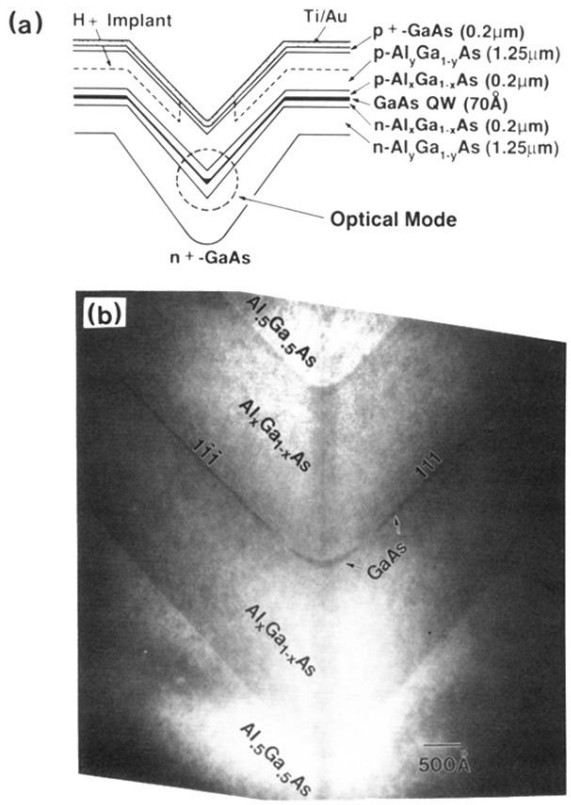


FIG. 1. Cross sections of GaAs/AlGaAs quantum wire heterostructure. (a) Schematic illustration; (b) dark-field transmission electron micrograph.